

---

# Opponent Modelling with Local Information Variational Autoencoders

---

Georgios Papoudakis

Filippos Christianos

Stefano V. Albrecht

School of Informatics  
University of Edinburgh

{g.papoudakis, f.christianos, s.albrecht}@ed.ac.uk

## Abstract

Modelling the behaviours of other agents (opponents) is essential for understanding how agents interact and making effective decisions. Existing methods for opponent modelling commonly assume knowledge of the local observations and chosen actions of the modelled opponents, which can significantly limit their applicability. We propose a new modelling technique based on variational autoencoders which uses only the local observations of the agent under control: its observed world state, chosen actions, and received rewards. The model is jointly trained with the agent’s decision policy using deep reinforcement learning techniques. We provide a comprehensive evaluation and ablation study in diverse multi-agent tasks, showing that our method achieves significantly higher returns than a baseline method which does not use opponent modelling, and comparable performance to an ideal baseline which has full access to opponent information.

## 1 Introduction

An important aspect in autonomous decision-making agents is the ability to reason about the unknown intentions and behaviours of other agents. Much research has been devoted to this *opponent modelling* problem [2], with recent works focused on the use of deep learning architectures for opponent modelling [10, 15, 26, 27].

A common assumption in current methods is that the modelling agent has access to the local information of the modelled agents, which may include their local observations of the environment state, their past actions, and possibly their received rewards. While it is certainly desirable to be able to observe an agent’s local context in order to reason about its past and future decisions, in practice such an assumption may be too restrictive. Agents may only have a limited view of their surroundings, communication with other agents may not be feasible or reliable [33], and knowledge of the perception system of other agents may not be available [8]. In such cases, an agent must reason with only locally available information.

We consider the following question: *Can effective opponent modelling be achieved using only the locally available information of the modelling agent?* A strength of deep learning techniques is their ability to identify informative features in data. Here, we use deep learning techniques to extract informative features from a stream of local observations for the purposes of opponent modelling.

Specifically, we consider multi-agent settings in which we control one agent which must learn to interact with a given set of opponent agents (we use the term “opponent” in a neutral sense) as well as generalise to previously unseen opponents. We propose an opponent modelling method which is able to extract a compact yet informative representation of opponents given only the local information of the controlled agent, which includes its local state observations, past actions, and rewards. To this end, we use an encoder-decoder architecture based on variational autoencoders (VAE) [19]. The VAE model is trained to replicate opponent actions and observations from the local information only,

forcing the recurrent encoder network to identify informative embeddings from the stream of local observations. After training, only the encoder component is retained which generates embeddings using local information (similar to recent ideas based on centralised training with decentralised execution [21]). The learned embeddings condition the policy of the controlled agent in addition to its local observation. We train the decision policy and opponent model jointly using reinforcement learning (RL), allowing us to trade-off the VAE training objective with reward maximisation.

We evaluate our proposed methodology in two benchmark environments used in multi-agent systems research, the multi-agent particle environment [24] and level-based foraging [3]. Our results support the idea that effective opponent modelling can be achieved using only local information: the same RL algorithm generally achieved higher average returns when combined with our opponent embeddings than without, and in some cases the average returns are comparable to those achieved by an ideal baseline which has full access to the opponent information. We also evaluate the method’s ability to generalise to opponents not seen during training, and provide an ablation study on the different types of local information used by the encoder.

## 2 Related Work

**Learning Opponent Models:** We are interested in opponent modelling methods that use neural networks to learn representations of the opponents. He et al. [15] proposed a method which learns a modelling network to reconstruct an opponent’s actions given the opponent’s observations. Raileanu et al. [27] developed an algorithm for learning to infer an opponents’ intentions using the policy of the controlled agent. Grover et al. [10] proposed an encoder-decoder method for modelling the opponent’s policy. The encoder learns a point-based representation of different opponent trajectories, and the decoder learns to reconstruct the opponent’s policy. In addition, the authors introduced an objective to separate embeddings of different agents into different clusters. Rabinowitz et al. [26] proposed the Theory of mind Network (TomNet), which learns embedding-based representations of opponents for meta-learning. Tacchetti et al. [34] proposed relational forward models to model opponents using graph neural networks. A common assumption in these methods, which our work aims to eliminate, is that the modelling agent has full access to the opponent’s local information, including their observations, chosen actions, and received rewards.

**Representation Learning in Reinforcement Learning:** Another related topic which has received significant attention is representation learning in RL. Using unsupervised learning techniques to learn low-dimensional representations of the environment state has led to significant improvements in RL. Ha and Schmidhuber [13] proposed a VAE-based model and a forward model to learn state representations of the environment. Hausman et al. [14] learned task embeddings and interpolated them to solve more difficult tasks. Igl et al. [17] used a VAE model for learning state representations in partially-observable environments. Gupta et al. [12] proposed a model which learns Gaussian embeddings to represent different tasks during meta-training and manages to quickly adapt to new task during meta-testing. Gregor et al. [9] developed a VAE-based model for long-term state predictions. The work of Schulze et al. [31] is closely related, where the authors proposed a recurrent VAE model which receives as input the observation, action, reward of the controlled agent and learns a variational distribution of tasks. Rakelly et al. [28] used representations from an encoder for off-policy meta-RL. Note that all of these methods were designed for learning representations of tasks or properties of the environment. In contrast, our approach focuses on learning representations of opponents in multi-agent systems.

## 3 Technical Preliminaries

### 3.1 Reinforcement Learning

We model the decision problem as a Markov Decision Processes (MDP). An MDP consists of a set of states  $\mathcal{S}$ , a set of actions  $\mathcal{A}$ , a transition function,  $P(s'|s, a)$ , specifying the probability of the next state,  $s'$ , after taking action  $a$  in state  $s$ , and a reward function,  $r(s', a, s)$ , which returns a scalar value conditioned on two consecutive states and the intermediate action. A policy function is used to choose an action in given a state, which we assume can be stochastic,  $a \sim \pi(a|s)$ . Given a policy  $\pi$ , the state-value function is defined as  $V(s_t) = \mathbb{E}_\pi[\sum_{i=t}^H \gamma^{i-t} r_t | s = s_t]$  and the action-value (Q-value) function  $Q(s_t, a_t) = \mathbb{E}_\pi[\sum_{i=t}^H \gamma^{i-t} r_t | s = s_t, a = a_t]$ , where  $0 \leq \gamma \leq 1$  is the discount factor and

$H$  is the finite horizon of the episode. RL methods aim to compute an optimal policy that maximises the state value functions.

There is a large number of RL algorithms. In this work, we will use an algorithm called Synchronous Advantage Actor-Critic (A2C) [4, 23]. A2C is an on-policy actor-critic algorithm which uses parallel environment copies to break the correlation between consecutive experience samples. Assuming a policy  $\pi_\theta$  and value network  $V_\phi$  with parameters  $\theta$  and  $\phi$ , respectively, the actor-critic parameters are optimised via

$$\min_{\theta, \phi} \mathbb{E}_B [-\hat{A} \log \pi_\theta(a|s) + \frac{1}{2}(r + \gamma V_\phi(s') - V_\phi(s))^2] \quad (1)$$

where  $B$  is the batch of trajectories and  $\hat{A}$  is the advantage term.

### 3.2 Variational Autoencoder

Consider samples from a dataset  $x \in \mathcal{X}$  which are generated from some hidden (latent) random variable  $z$  based on a generative distribution  $p_u(x|z)$  with unknown parameter  $u$ , and a prior distribution on the latent variables which we assume to be Gaussian with zero mean and unit variance,  $p(z) = \mathcal{N}(z; \mathbf{0}, \mathbf{I})$ . We seek to approximate the true posterior  $p(z|x)$  with a variational parametric distribution  $q_w(z|x) = \mathcal{N}(z; \mu, \Sigma, w)$ . Kingma and Welling [19] proposed the Variational Autoencoder (VAE) to learn this distribution. Starting with the Kullback-Leibler (KL) divergence from the approximate to the true posterior,  $D_{\text{KL}}(q_w(z|x)||p(z|x))$ , the lower bound on the evidence  $\log p(x)$  (ELBO) is derived as:

$$\log p(x) \geq \mathbb{E}_{z \sim q_w(z|x)} [\log p_u(x|z)] - D_{\text{KL}}(q_w(z|x)||p(z)) \quad (2)$$

Maximising the ELBO leads to minimisation of the KL divergence from the approximate to the true posterior. The architecture consists of two neural networks: the encoder which receives a sample  $x$  and generates the Gaussian variational distribution  $p(z|x; w)$ ; and the decoder which receives a sample from the Gaussian variational distribution and reconstructs the generative distribution  $p_u(x|z)$ . The architecture is trained using the reparameterisation trick [19]. Higgins et al. [16] proposed  $\beta$ -VAE, which uses  $\beta_{\text{VAE}} > 0$  to regularise the two terms of the ELBO.

## 4 Approach

### 4.1 Problem Formulation

We consider a Markov game [20] which consists of  $N$  agents  $\mathbb{I} = \{1, 2, \dots, N\}$ , a state space  $\mathcal{S}$ , the joint action space  $\mathcal{A} = \mathcal{A}_1 \times \dots \times \mathcal{A}_N$ , a transition function  $P : \mathcal{S} \times \mathcal{A} \times \mathcal{S} \rightarrow [0, 1]$  specifying the transition probabilities between states given a joint action, and for each agent  $i \in \mathbb{I}$  a reward function  $r_i : \mathcal{S} \times \mathcal{A} \times \mathcal{S} \rightarrow \mathbb{R}$ . We consider partially observable settings, where each agent  $i$  has access only to its local observation  $o_i \subset s \in \mathcal{S}$  and reward  $r_i$ . We denote the agent under our control by 1, and the other agents by  $-1$  where for notational convenience we will treat the other agents as a single “combined” agent with joint observations  $o_{-1}$  and actions  $a_{-1}$ .

We assume a set of opponent policies,  $\Pi_{-1} = \{\pi_{-1}^k | k = 1, \dots, K\}$ , which may be defined manually (heuristic) or pretrained using RL. Each opponent policy determines the opponent’s actions as a mapping  $\pi_{-1}^k(o_{-1})$  from the opponent’s local observation  $o_{-1}$  to a distribution over actions  $a_{-1}$ . Our goal is to find a policy  $\pi_\theta$  parameterised by  $\theta$  for agent 1 which maximises the average return against opponents from the training set  $\Pi_{-1}$ , assuming that each opponent policy is initially equally probable and fixed during an episode (the objective can be modified to use non-uniform distributions):

$$\arg \max_{\theta} \mathbb{E}_{\pi_\theta, \pi_{-1} \sim \mathcal{U}(\Pi_{-1})} \left[ \sum_{t=1}^H \gamma^t r_{1,t} \right] \quad (3)$$

where  $r_{1,t}$  is the reward received by agent 1 at time  $t$ ,  $H$  is the episode length (horizon), and  $\gamma \in (0, 1)$  is a discount factor. We seek to learn such a policy while still being able to generalise to unknown opponents (not in  $\Pi_{-1}$ ). Section 5 gives further details on how we test generalisation capabilities.

## 4.2 Local Information Variational Autoencoders

We denote by  $\tau_{-1} = \{o_{-1,t}, a_{-1,t}\}_{t=0}^{t=H}$  an opponent trajectory where  $o_{-1,t}$  and  $a_{-1,t}$  are the opponent's observation and action at time step  $t$  in the trajectory, up to horizon  $H$ . These trajectories are generated from the opponent policies in  $\Pi_{-1}$ , which are represented in a latent (or *embedding*) space  $\mathcal{Z}$  and for which we assume there exists an unknown generative model  $p_{\mathbf{u}}(\tau_{-1}|z), z \in \mathcal{Z}$ . The latent variable  $z$  contains information about the trajectory of the opponent. Our approach is to solve the problem defined in Section 4.1 by performing reinforcement learning in the joint space of the observation space of our agent and the latent space of the opponent. We aim to approximate the unknown posterior,  $p(z|\tau_{-1})$ , using a variational Gaussian distribution  $\mathcal{N}(\mu, \Sigma; \mathbf{w})$  with parameters  $\mathbf{w}$ . As a result, during execution, we can sample the latent variable from the approximate posterior  $z \sim \mathcal{N}(z; \mu, \Sigma; \mathbf{w})$ .

In Sections 1 and 2, it was noted that most agent modelling methods assume access to the opponent's observations and actions both during training and execution. To eliminate this assumption, we propose a VAE that uses a parametric variational distribution which is conditioned on the observation-action-reward triplet of the agent under our control and a variable  $d$  indicating whether the episode has terminated;  $q_{\mathbf{w}}(z|\tau_1 = (o_{1,1:t}, a_{1,1:t-1}, r_{1,1:t-1}, d_{1,1:t-1}))$ . Specifically, we approximate the true posterior that is conditioned on opponent's information, with a variational distribution that only depends on local information. The use of such local information in a recurrent fashion has been successfully used in meta-RL settings [5, 35]. We start by writing the KL divergence from the approximate to the true posterior:

$$D_{\text{KL}}(q_{\mathbf{w}}(z|\tau_1)||p(z|\tau_{-1})) = \mathbb{E}_{z \sim q_{\mathbf{w}}(z|\tau_1)} [\log q_{\mathbf{w}}(z|\tau_1) - \log p(z|\tau_{-1})] \quad (4)$$

By following the works of Kingma and Welling [19] and Higgins et al. [16] and using the Jensen inequality, the negative evidence lower bound can be written as:

$$\mathcal{L}(\tau_1, \tau_{-1}; \mathbf{w}, \mathbf{u}) = -\mathbb{E}_{z \sim q_{\mathbf{w}}(z|\tau_1)} [\log p_{\mathbf{u}}(\tau_{-1}|z)] + \beta_{\text{VAE}} D_{\text{KL}}(q_{\mathbf{w}}(z|\tau_1)||p(z)) \quad (5)$$

From Equation 5, we observe that the variational distribution depends only on locally available information. Since during execution only the encoder is required to generate the opponent's model, this approach removes the assumption that access to the opponent's observations and actions is available during execution. At each time step  $t$ , the recurrent encoder network generates a latent sample  $z_t$ , which is conditioned on the information of the agent under control  $(o_{1,1:t}, a_{1,1:t-1}, r_{1,1:t-1}, d_{1,1:t-1})$ , until time step  $t$ .

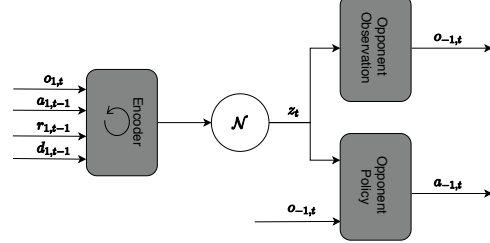


Figure 1: Diagram of LIOM architecture.

The lower bound also consists of the reconstruction loss of the opponent's trajectory which involves the observation and actions of the opponent. The opponent's observation depends on the dynamics of the environment. The opponent's action at each time step depends on its observation and the opponent's identity, which is represented by the latent variable  $z$ . Therefore, the decoder consists of two fully-connected feed-forward networks.

$$\begin{aligned} \log p_{\mathbf{u}}(\tau_{-1}|z) &= \sum_{t=1}^H \log p(o_{-1,t}|z_t) p_{\mathbf{u}}(a_{-1,t}|o_{-1,t}, z_t) = \\ &= \sum_{t=1}^H [\log p_{\mathbf{u}}(o_{-1,t}|z_t) + \log p_{\mathbf{u}}(a_{-1,t}|o_{-1,t}, z_t)] \end{aligned} \quad (6)$$

From Equation 6, we observe that conditioned on the latent variable, the decoder reconstructs the opponent's observation and the opponent's action given the opponent's observation. Intuitively,  $z_t$  encodes the type of policy used by the opponent at the current episode and its observation at time step  $t$ . Figure 1 illustrates the proposed VAE. We refer to this method as **LIOM** (Local Information Opponent Modelling). LIOM uses the information of both the controlled agent and opponent during training, but during execution only the information of the controlled agent is used.

### 4.3 Reinforcement Learning Training

We use the latent variable  $z$  augmented with our agent’s observation to condition the policy of our agent, which is optimised using RL. Consider the augmented observation space  $\mathcal{O}' = \mathcal{O} \times \mathcal{Z}$ , where  $\mathcal{O}$  is the original observation space of our agent in the Markov game, and  $\mathcal{Z}$  is the representation space of the opponent models. The advantage of learning the policy on  $\mathcal{O}'$  compared to  $\mathcal{O}$  is that the policy can adapt to different  $z \in \mathcal{Z}$ . We optimise the proposed VAE model jointly with the policy of the controlled agent, using the A2C algorithm (cf. Sec. 3.1). Note that other RL algorithm could be used instead of A2C. The input to the actor and critic are the local observation and a the mean of the variational distribution. We do not back-propagate the gradient from the actor-critic loss (Equation 1) to the parameters of the encoder. Note that in contrast to the works of Duan et al. [5], Wang et al. [35], we reset the recurrent network’s hidden state at the beginning of each episode and we do not assume that our trained agent has a number of adaptation episodes. Additionally, we subtract the policy entropy from the policy gradient loss to encourage exploration [23]. Given a batch  $B$  of collected trajectories in the environment, the update equation for our proposed method is the following:

$$\min_{\phi, \theta, w, u} \mathbb{E}_B \left[ \frac{1}{2} (r_1 + \gamma V_\phi(o'_1, \mu(z')) - V_\phi(o_1, \mu(z)))^2 - \hat{A} \log \pi_\theta(a_1|o_1, \mu(z)) - \beta H(\pi_\theta(a_1|o_1, \mu(z))) \right. \\ \left. - \lambda_1 \log p_u(o_{-1}|z) - \lambda_2 \log p_u(a_{-1}|o_{-1}, z) + \beta_{\text{VAE}} D_{\text{KL}}(q_w(z|\tau_1) \| p(z)) \right] \quad (7)$$

The pseudocode of LIOM is given in Appendix A. Intuitively, at the beginning of each episode, LIOM starts with an uninformative posterior which is equal to the prior (isotropic Gaussian) over the possible opponents. At each time step, the agent interacts with the environment and the opponent and updates the posterior over opponents based on the local information that it perceives.

## 5 Experiments

### 5.1 Experimental Framework

We evaluate the proposed method in the speaker-listener and double-speaker listener environments [24] and the level-based foraging environment [1, 3]. Brief descriptions are provided below. More detailed descriptions and instances of the environments are provided in Appendix B. The implementation details are provided in appendix C.

**Speaker-listener:** the environment consists of two agents, called speaker and listener, as well as three designated landmarks. Each agent and landmark has one of three possible colours – red, green, blue – which are assigned randomly at the beginning of each episode. The task of the listener is to navigate to the landmark that has the same colour as the listener. However, the colour of the listener can only be observed by the speaker. The listener observes the communicated message of the speaker and has to navigate to the correct landmark.

**Double speaker-listener:** the environment consists of two agents and three designated landmarks, similarly to the speaker-listener environment. The only difference is that both agents are simultaneously speakers and listeners. Therefore, at the beginning of the episode, each agent has a colour that can only be observed by the other agent. Each agent must learn both to communicate a message to the other agent as well as navigate to the correct landmark.

**Level-based foraging:** the environment is a  $20 \times 20$  grid-world, consisting of two agents and four food locations. The agents and the foods are assigned random levels at the beginning of an episode. The goal is for the agents to collect all foods. Agents can either move in one of the four directions or attempt a load. A group of one or more agents successfully load a food if the agents are positioned in the adjacent cells to the food and if the sum of the agents’ levels is at least as high as the food’s level.

In each environment, we create ten different opponent policies, of which eight are used for training (in set  $\Pi_{-1}$ ) and two for testing strong generalisation as detailed below. In speaker-listener, we control the listener, and we create ten different speakers using different communication messages for different colours. In double speaker-listener, we create a diverse set of opponents that have different communication messages similar to speaker-listener, while they learn to navigate using the MADDPG algorithm [21], with different initial random seeds. For level-based foraging, we created ten different

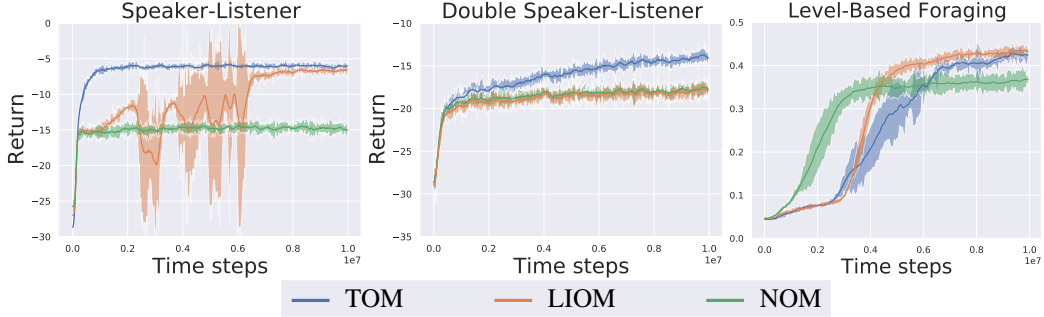


Figure 2: Episodic return during training against opponent policies from  $\Pi_{-1}$ .

opponents: four using heuristics such as moving to the closest food or closest level-compatible food, and six using MADDPG with different initial seeds leading to different trained policies.

We use agent generalisation graphs [11] to evaluate the generalisation capabilities of the proposed method. We evaluate two types of generalisations in this work. First, we evaluate the episodic returns against opponent policies used for training,  $\Pi_{-1}$ , which Grover et al. [11] call "weak generalisation". During weak generalisation, the opponent policies are the same as used during training and only the initial state of the MDP differs. Secondly, we evaluate against unknown opponents not used during training, which is called "strong generalisation". During strong generalisation, different opponent policies and initial MDP states are used for evaluation.

## 5.2 Episodic Returns in Training

We compare our method against two baselines, which are indicative of the upper and the lower performance bound of our method. For the upper bound, we propose a VAE-based opponent model which is trained on the trajectories of the opponents. The encoder of the VAE receives as input the observation and the action of the opponent and infers the opponent model  $z$ . We call this baseline TOM (True Opponent Model). TOM approximates the latent opponent identity distribution using a variational distribution that is conditioned on the trajectory of the opponent. We optimise the opponent representation along with the reinforcement learning objective similarly to LIOM. Note that TOM has access to opponent's information both during training and execution. The lower baseline that we use is called No Opponent Model (NOM). NOM uses the A2C algorithm without any model of the opponent.

Figure 2 shows the episodic returns for the three methods in all three environments. The lines shown in our results plots show the average return over five runs with different initial seeds, and the shadowed part represents the 95% confidence interval. We evaluate the methods every 1000 training episodes for 100 episodes. During the evaluation, we compute the mean of the variational distribution at each time step, and the agent follows the stochastic policy. We found that sampling the action from the policy distribution leads to significantly higher returns compared to following the greedy policy. We observe that LIOM's episodic returns are closer to TOM than NOM in the speaker-listener environment. This shows that LIOM can successfully learn opponent models using only locally available information. In the double speaker-listener, the returns of LIOM and NOM are similar, indicating that the model does not contribute towards increasing the returns. In the level-based foraging environment, we observe that LIOM's performance becomes similar or better than TOM's performance. This happens because the level-based foraging is a fully-observable environment, but it also highlights that LIOM can perform similar to the upper baseline without observing the actions of the opponent. In some environments, in the first half of the training, the performance of LIOM or TOM is low or highly variable (spikes) compared to the performance of NOM. This results from the fact that the agent explores the environment and the encoder has to adapt to newly observed trajectories and as a result the output of the encoder has large variation leading to low returns. At the second half of the training, the encoder has already been trained on most of the possible trajectories, producing stable representations and A2C is able to increase the returns.

Environment	TOM	LIOM	NOM
Speaker-listener	-6.15	-6.94	-19.39
Double speaker-listener	-15.93	-20.82	-28.24
Level-based foraging	0.31	0.35	0.27

Table 1: Average episodic return of the trained agent against unknown opponent policies.

### 5.3 Generalisation to Unknown Opponents

We evaluate the ability of trained models and policies to generalise to opponents which were not accessible during training, i.e. strong generalisation. Table 1 shows the average returns of the trained policies for the controlled agent against the unknown opponent policies in all environments for 1000 episodes and five different seeds. In speaker-listener the returns of TOM and LIOM during strong generalisation remain similar to the returns during weak generalisation. We observe that the average episodic returns of LIOM decrease marginally during strong generalisation compared to NOM in the double speaker-listener, despite that their episodic returns during weak generalisation are similar. As a result, we conclude that NOM only learns to memorise observations, while LIOM learns an efficient opponent model that can generalise to unseen opponents. In the level-based foraging, LIOM generalises better to unknown opponent compared to TOM and NOM.

### 5.4 Encoder Evaluation

We analyse the embeddings learned by LIOM’s encoder. Figure 3 presents the first two principal components of the mean of the variational distribution at the 20th time step of the episode for all opponents in  $\Pi_{-1}$ . In speaker-listener and double speaker-listener, we observe that three different clusters are created, representing the three different colours that the opponent observes. We observe that the controlled agent learns to perfectly identify the underlying hidden information in the observation of the opponent. In level-based foraging, seven clusters are created which represent different intention or observations of the opponent. Note that the embeddings are not clustered based on the opponent identities but based on the selected actions and private observations, which means that different opponents may be embedded in the same region.

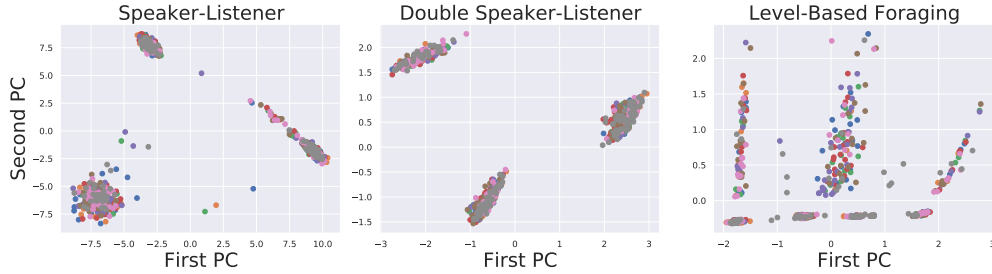


Figure 3: First and second principal components of the learned opponent representations. Points represent individual episodes, colours represent the different opponent policies in  $\Pi_{-1}$ .

### 5.5 Decoder Evaluation

The decoder of LIOM consists of two networks, one for reconstructing the opponent’s observation and one for reconstructing the opponent’s actions. We train the two networks to maximise the log-likelihood of the opponent’s trajectory. We found that weighting the importance of each term with the factors  $\lambda_1$  and  $\lambda_2$  improves the returns that LIOM achieves. In Figure 4, we present the average returns that LIOM achieves with respect to  $\frac{\lambda_1}{\lambda_2}$  ratio during weak generalisa-

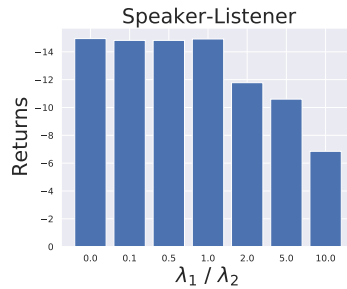


Figure 4: Returns with respect to  $\frac{\lambda_1}{\lambda_2}$ .

tion. In the speaker-listener environment, inferring the observation of the speaker is more important than inferring its action, because it directly informs the listener about its colour. As a result, large values of the ratio lead to better returns. Overall, the values of  $\lambda_1$  and  $\lambda_2$  that maximise the returns that LIOM can achieve depend on the properties of the environment and have to be optimised separately for each case.

## 5.6 Ablation Study on LIOM Inputs

Our full method utilises the observation, action, reward, and termination sequence of the controlled agent to generate the opponent model. To evaluate the impact of different types of input data, we use different combinations of inputs in the encoder and compare the episodic returns. Figure 5 presents the average episode return for three different cases: LIOM (full), LIOM using only observations and actions, and LIOM using only observations and rewards.

From Figure 5, we observe that in the speaker-listener environment the most important component is the reward. Due to the dense reward signal given in the environment, our agent can essentially learn to follow the direction of reward increase via the learned embeddings (this information is not available to LIOM(Obs,Act)). In the double speaker-listener and in the lb-foraging, the performance is not significantly affected by the absence of either the reward or the previous action. Our experiments indicate that LIOM is robust with respect to different input data in the encoder in two of the tested environments.

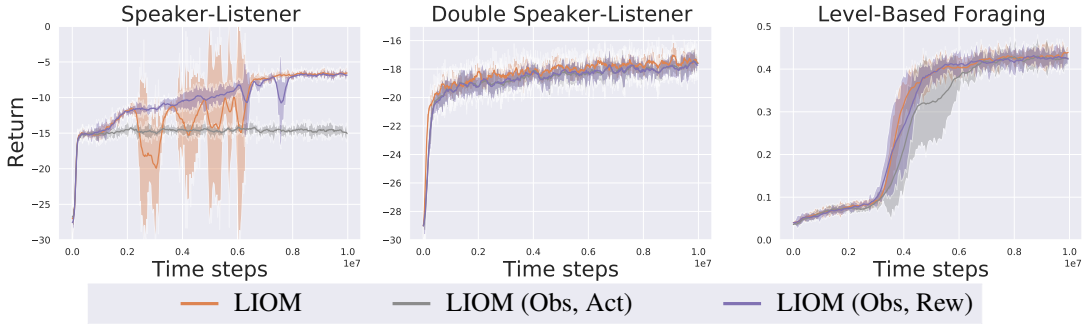


Figure 5: Episodic return during training against opponent policies from  $\Pi_{-1}$  for different combinations of input data for the encoder.

## 6 Conclusion

We proposed a new opponent modelling approach, LIOM, which jointly trains a VAE-based opponent model with a decision policy for the agent under control, such that the resulting opponent model is conditioned only on the local observations of the controlled agent. Our method is simple and efficient and can be combined with different RL algorithms. Additionally, LIOM is agnostic to the type of interactions in the environment (cooperative, competitive, mixed) and can model an arbitrary number of opponents simultaneously. Our results show that LIOM can significantly improve the episodic return that the controlled agent achieves over methods that do not use opponent modelling as well as generalise efficiently to unknown opponents. Compared to baseline methods that require access to opponent trajectories during execution, we observed a relatively small decrease in performance of LIOM in our specific test environments. To the best of our knowledge, this is the first study showing that effective opponent modelling can be achieved without requiring access to opponent observations. We hope that this first study of opponent modelling using only local information will motivate future research in this direction. Further research on how such models could be used for non-stationary opponents would be of interest. In particular, we plan on investigating two scenarios; the first is multi-agent deep RL, where different agents are learning concurrently leading to non-stationarity in the environment, which prevents the agents from learning optimal policies [25]. Secondly, we would like to explore notions of “safety” to handle opponents which aim to deceive and exploit the opponent model [6, 7, 32].



## References

- [1] Stefano V Albrecht and Subramanian Ramamoorthy. A game-theoretic model and best-response learning method for ad hoc coordination in multiagent systems. In *International Conference on Autonomous Agents and Multi-Agent Systems*, 2013.
- [2] Stefano V Albrecht and Peter Stone. Autonomous agents modelling other agents: A comprehensive survey and open problems. *Artificial Intelligence*, 258, 2018.
- [3] S.V. Albrecht and P. Stone. Reasoning about hypothetical agent behaviours and their parameters. In *International Conference on Autonomous Agents and Multi-Agent Systems*, 2017.
- [4] Prafulla Dhariwal, Christopher Hesse, Oleg Klimov, Alex Nichol, Matthias Plappert, Alec Radford, John Schulman, Szymon Sidor, Yuhuai Wu, and Peter Zhokhov. Openai baselines. <https://github.com/openai/baselines>, 2017.
- [5] Yan Duan, John Schulman, Xi Chen, Peter L Bartlett, Ilya Sutskever, and Pieter Abbeel. RL<sup>2</sup>: Fast reinforcement learning via slow reinforcement learning. *arXiv preprint arXiv:1611.02779*, 2016.
- [6] Sam Ganzfried and Tuomas Sandholm. Game theory-based opponent modeling in large imperfect-information games. In *International Conference on Autonomous Agents and Multiagent Systems*, 2011.
- [7] Sam Ganzfried and Tuomas Sandholm. Safe opponent exploitation. *ACM Transactions on Economics and Computation (TEAC)*, 2015.
- [8] P.J. Gmytrasiewicz and P. Doshi. A framework for sequential planning in multiagent settings. *Journal of Artificial Intelligence Research*, 2005.
- [9] Karol Gregor, George Papamakarios, Frederic Besse, Lars Buesing, and Theophane Weber. Temporal difference variational auto-encoder. *International Conference on Learning Representations*, 2019.
- [10] Aditya Grover, Maruan Al-Shedivat, Jayesh K Gupta, Yura Burda, and Harrison Edwards. Learning policy representations in multiagent systems. *International Conference on Machine learning*, 2018.
- [11] Aditya Grover, Maruan Al-Shedivat, Jayesh K Gupta, Yuri Burda, and Harrison Edwards. Evaluating generalization in multiagent systems using agent-interaction graphs. In *International Conference on Autonomous Agents and Multiagent Systems*, 2018.
- [12] Abhishek Gupta, Russell Mendonca, YuXuan Liu, Pieter Abbeel, and Sergey Levine. Meta-reinforcement learning of structured exploration strategies. In *Advances in Neural Information Processing Systems*, 2018.
- [13] David Ha and Jürgen Schmidhuber. World models. *arXiv preprint arXiv:1803.10122*, 2018.
- [14] Karol Hausman, Jost Tobias Springenberg, Ziyu Wang, Nicolas Heess, and Martin Riedmiller. Learning an embedding space for transferable robot skills. *International Conference on Learning Representations*, 2018.
- [15] He He, Jordan Boyd-Graber, Kevin Kwok, and Hal Daumé III. Opponent modeling in deep reinforcement learning. In *International Conference on Machine Learning*, 2016.
- [16] Irina Higgins, Loic Matthey, Arka Pal, Christopher Burgess, Xavier Glorot, Matthew Botvinick, Shakir Mohamed, and Alexander Lerchner. beta-vae: Learning basic visual concepts with a constrained variational framework. *International Conference on Learning Representations*, 2017.
- [17] Maximilian Igl, Luisa Zintgraf, Tuan Anh Le, Frank Wood, and Shimon Whiteson. Deep variational reinforcement learning for pomdps. In *International Conference on Machine Learning*, pages 2122–2131, 2018.

- [18] Diederik P Kingma and Jimmy Ba. Adam: A method for stochastic optimization. *arXiv preprint arXiv:1412.6980*, 2014.
- [19] Diederik P Kingma and Max Welling. Auto-encoding variational bayes. *International Conference on Learning Representations*, 2014.
- [20] Michael L Littman. Markov games as a framework for multi-agent reinforcement learning. In *Machine Learning Proceedings 1994*. Elsevier, 1994.
- [21] Ryan Lowe, Yi Wu, Aviv Tamar, Jean Harb, OpenAI Pieter Abbeel, and Igor Mordatch. Multi-agent actor-critic for mixed cooperative-competitive environments. In *Advances in Neural Information Processing Systems*, 2017.
- [22] Andrew L Maas, Awni Y Hannun, and Andrew Y Ng. Rectifier nonlinearities improve neural network acoustic models. In *International Conference on Machine Learning*, 2013.
- [23] Volodymyr Mnih, Adria Puigdomenech Badia, Mehdi Mirza, Alex Graves, Timothy Lillicrap, Tim Harley, David Silver, and Koray Kavukcuoglu. Asynchronous methods for deep reinforcement learning. In *International Conference on Machine Learning*, pages 1928–1937, 2016.
- [24] Igor Mordatch and Pieter Abbeel. Emergence of grounded compositional language in multi-agent populations. *arXiv preprint arXiv:1703.04908*, 2017.
- [25] Georgios Papoudakis, Filippos Christianos, Arrasy Rahman, and Stefano V Albrecht. Dealing with non-stationarity in multi-agent deep reinforcement learning. *arXiv preprint arXiv:1906.04737*, 2019.
- [26] Neil C Rabinowitz, Frank Perbet, H Francis Song, Chiyuan Zhang, SM Eslami, and Matthew Botvinick. Machine theory of mind. *International Conference on Machine Learning*, 2018.
- [27] Roberta Raileanu, Emily Denton, Arthur Szlam, and Rob Fergus. Modeling others using oneself in multi-agent reinforcement learning. *arXiv preprint arXiv:1802.09640*, 2018.
- [28] Kate Rakelly, Aurick Zhou, Deirdre Quillen, Chelsea Finn, and Sergey Levine. Efficient off-policy meta-reinforcement learning via probabilistic context variables. *International Conference on Machine Learning*, 2019.
- [29] Jürgen Schmidhuber and Sepp Hochreiter. Long short-term memory. *Neural Computation*, 1997.
- [30] John Schulman, Philipp Moritz, Sergey Levine, Michael Jordan, and Pieter Abbeel. High-dimensional continuous control using generalized advantage estimation. *arXiv preprint arXiv:1506.02438*, 2015.
- [31] S Schulze, S Whiteson, L Zintgraf, M Igl, Yarin Gal, K Shiarlis, and K Hofmann. Varibad: a very good method for bayes-adaptive deep rl via meta-learning. In *International Conference on Learning Representations*, 2020.
- [32] Yoav Shoham, Rob Powers, and Trond Grenager. If multi-agent learning is the answer, what is the question? *Artificial intelligence*, 171(7):365–377, 2007.
- [33] P. Stone, G.A. Kaminka, S. Kraus, and J.S. Rosenschein. Ad hoc autonomous agent teams: collaboration without pre-coordination. In *Proceedings of the 24th AAAI Conference on Artificial Intelligence*, 2010.
- [34] Andrea Tacchetti, H Francis Song, Pedro AM Mediano, Vinicius Zambaldi, Neil C Rabinowitz, Thore Graepel, Matthew Botvinick, and Peter W Battaglia. Relational forward models for multi-agent learning. *arXiv preprint arXiv:1809.11044*, 2018.
- [35] Jane X Wang, Zeb Kurth-Nelson, Dhruva Tirumala, Hubert Soyer, Joel Z Leibo, Remi Munos, Charles Blundell, Dharshan Kumaran, and Matt Botvinick. Learning to reinforcement learn. *arXiv preprint arXiv:1611.05763*, 2016.

## A Pseudocode of LIOM

Algorithm 1 shows the pseudocode of LIOM.

---

### Algorithm 1 Pseudocode of the LIOM algorithm

---

```

for  $m = 1, \dots, M$  episodes do
  Reset the hidden state of the encoder LSTM
  Sample  $E$  opponent policies from  $\Pi_{-1}$ 
  Create  $E$  parallel environments and
  gather initial observations
   $a_{1,0}, r_{1,0}, d_{1,0} \leftarrow$  zero vectors
  for  $t = 1, \dots, H$  do
    for every environment  $e$  in  $E$  do
      Get observations  $o_{1,t}$  and  $o_{-1,t}$ 
      Sample  $z_t \sim q(z|o_{1,t}, a_{1,t-1}, r_{1,t-1}, d_{1,t-1})$ 
      Sample action  $a_{1,t} \sim \pi(o_{1,t}, z_t)$ 
      Sample opponent action  $a_{-1,t} \sim \pi_{-1}(o_{-1,t})$ 
      Perform the actions and get  $o_{1,t+1}, r_{1,t}, d_{1,t}$ 
    end for
    if  $t \bmod \text{update\_frequency} = 0$  then
      Gather the sequences of all  $E$  environments in a single batch  $B$ 
      Perform a gradient step to minimise (7)
    end if
  end for
end for

```

---

## B Evaluation Environments

**Speaker-listener:** the environment consists of two agents, called speaker and listener, as well as three designated landmarks. Each agent and landmark has one of three possible colours – red, green, blue – which are assigned randomly at the beginning of each episode. The task of the listener is to navigate to the landmark that has the same colour as the listener. However, the colour of the listener can only be observed by the speaker, thus the speaker has to learn to communicate the correct colour to the listener. The speaker observes the colour of the goal landmark as a one-hot encoded vector and outputs a 5-bit binary communication message as an action. The listener observes the communicated message of the previous time step and can choose to navigate using the actions forward, backward, right, left, no-op. The reward at each time step is the negative Euclidean distance between the listener and the correct landmark.

**Double speaker-listener:** the environment consists of two agents and three designated landmarks, similarly to the speaker-listener environment. The only difference is that both agents are simultaneously speakers and listeners. Therefore, at the beginning of the episode, each agent has a colour that can only be observed by the other agent. Each agent must learn both to communicate a message to the other agent as well as navigate to the correct landmark. Each agent performs both actions from the previous environment; it communicates the opponents goal landmark and navigates to its own. The reward at each time step is the negative average Euclidean distance between each agent and the corresponding correct landmark.

**Level-based foraging:** the environment is a  $20 \times 20$  grid-world, consisting of two agents and four food locations. The agents and the foods are assigned random levels at the beginning of an episode. The goal is for the agents to collect all foods. Agents can either move in one of the four directions or attempt a load. A group of one or more agents successfully load a food if the agents are positioned in the adjacent cells to the food and if the sum of the agents' levels is at least as high as the food's level. The controlled agent has to learn to cooperate to load foods with a high level and at the same time act greedily for foods that have lower levels. The environment has sparse rewards, representing the contribution of the agent in the gathering all foods in the environment. For example, if the agent receives a food with level 2, and there are another three foods with levels 1, 2 and 3 respectively, the

reward of the agent is  $2/(1 + 2 + 2 + 3) = 0.25$ . Thus, the maximum cumulative reward that both agents can achieve is normalised to 1.

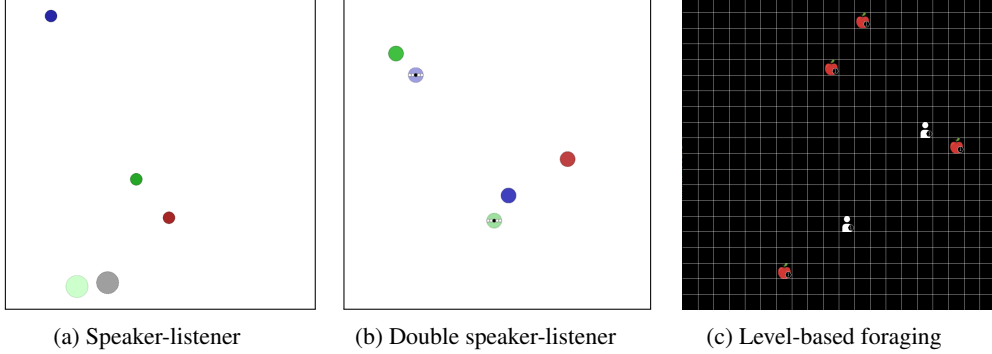


Figure 6: Multi-agent environments used in our evaluation.

## C Implementation Details

All feed-forward neural networks have 2 hidden layers with ReLU [22] activation function. The encoder consists of one LSTM [29] and a linear layer with ReLU activation function. All hidden layers consist of 128 nodes. The dimension of the latent variables is 8 for speaker-listener, 10 for double speaker-listener, and 5 for level-based foraging. The output of the decoder is passed through a softmax activation function to approximate the categorical opponent policy. For a continuous action space, a Gaussian distribution can be used. For the advantage computation, we use the Generalised Advantage Estimator [30] with  $\lambda_{GAE} = 0.95$ . We create 10 parallel environments to break the correlation between consecutive samples. The actor and the critic share all hidden layers. We use the Adam optimiser [18] with learning rate  $2 \times 10^{-4}$  and we clip the gradient norm to 0.5. In the speaker-listener and double speaker-listener, the factors are  $\lambda_1 = 1$  and  $\lambda_2 = 0.1$  and  $\beta_{VAE} = 0.1$ . In the level-based foraging, the factors are  $\lambda_1 = 1$  and  $\lambda_2 = 1$  and  $\beta_{VAE} = 1$ . We subtract the policy entropy from the actor loss [23] to ensure sufficient exploration. The entropy weight  $\beta$  is 0.01 for speaker-listener and double speaker-listener, and 0.001 for level-based foraging. We train for 10 million steps in all environments. The implementation of LIOM for the speaker-listener environment is provided in the supplementary material.